HHS Public Access

Author manuscript

Transplant Proc. Author manuscript; available in PMC 2016 February 17.

Published in final edited form as:

Transplant Proc. 2011 November ; 43(9): 3221–3225. doi:10.1016/j.transproceed.2011.09.009.

Assessment of Tissue-Engineered Islet Graft Viability by Fluorine Magnetic Resonance Spectroscopy

T.M. Suszynski, **E.S. Avgoustiniatos**, **S.A. Stein**, **E.J. Falde**, **B.E. Hammer**, and **K.K. Papas**

Schulze Diabetes Institute, Department of Surgery (T.M.S., E.S.A., S.A.S., E.J.F., K.K.P.) and Center for Interdisciplinary Applications in Magnetic Resonance, Department of Radiology (B.E.H.), University of Minnesota, Minneapolis, Minnesota, USA.

Abstract

Introduction—Despite significant progress in the last decade, islet transplantation remains an experimental therapy for a limited number of patients with type 1 diabetes. Tissue-engineered approaches may provide promising alternatives to the current clinical protocol and would benefit greatly from concurrent development of graft quality assessment techniques. This study was designed to evaluate whether viability of tissue-engineered islet grafts can be assessed using fluorine magnetic resonance spectroscopy (^{19}F-MRS), by the noninvasive measurement of oxygen partial pressure (pO_2) and the subsequent calculation of islet oxygen consumption rate (OCR).

Methods—Scaffolds composed of porcine plasma were seeded with human islets and perfluorodecalin. Each graft was covered with the same volume of culture media in a Petri dish. Four scaffolds were seeded with various numbers (0–8000) of islet equivalents (IE) aliquoted from the same preparation. After randomizing run order, grafts were examined by ^{19}F-MRS at 37°C using a 5T spectrometer and a single-loop surface coil placed underneath. A standard inversion recovery sequence was used to obtain characteristic ^{19}F spin-lattice relaxation times (T1), which were converted to steady-state average pO_2 estimates using a previously determined linear calibration (R^2 = 1.000). Each condition was assessed using replicate ^{19}F-MRS measurements (n = 6–8).

Results—Grafts exhibited IE dose-dependent increases in T1 and decreases in pO_2 estimates. From the difference between scaffold pO_2 estimates and ambient pO_2, the islet preparation OCR was calculated to be 95 ± 12 (mean ± standard error of the mean) nmol/(min · mg DNA) using theoretical modeling. This value compared well with OCR values measured using established methods for human islet preparations.

Conclusions—^{19}F-MRS can be used for noninvasive pre- and possibly posttransplant assessment of tissue-engineered islet graft viability by estimating the amount of viable, oxygen-consuming tissue in a scaffold.

Address reprint requests to Klearchos K. Papas, PhD, Associate Professor, Schulze Diabetes Institute, Department of Surgery, University of Minnesota, 420 Delaware Street SE, Mayo Mail Code 280, Minneapolis, MN 55455. papas006@umn.edu.

Widespread utilization of islet transplantation (ITx) in the treatment of type 1 diabetes has yet to be achieved[1–3] despite significant progress over the last decade.[4–9] Intraportal delivery of islets may not be the optimal approach. The development of tissue-engineered strategies for extrahepatic ITx may present a promising long-term opportunity.[10,11] Ultimately, the liver may not provide the best environment for healthy engraftment of transplanted islet tissue for a number of reasons that include but are not limited to: (1) higher concentrations of orally administered immunosuppressants,[12,13] which are known to impair normal insulin secretory function[14,15] and islet revascularization[16,17]; (2) intraportal thrombus formation and the associated inflammatory reaction, which are believed to contribute to early islet loss[18–20]; (3) poor reestablishment of the surrounding extracellular matrix, which is believed to adversely affect islet survival[21,22]; and (4) poor oxygenation due to the mixed arterial and portal circulation[23] and the presence of significant oxygen gradients within the hepatic parenchyma,[24] which are believed to be particularly important due to the poor capacity of islets to undergo anaerobic metabolism and their general susceptibility to hypoxic stress.[25-27]

Current efforts in islet graft tissue engineering have been accompanied by inconsistent outcomes when translated to small- or large-animal transplant models. These efforts may have been stunted by an inability to accurately assess graft quality both pre- and posttransplantation. Improved methods for quality assessment of islet products prior to transplantation have enabled more accurate characterization of islet viability and potency.[28] Many of the most promising methods involve quantification of oxygen consumption.[29–35] However, these techniques have yet to be extended to assessing the quality of tissue-engineered islet grafts. Herein we have presented preliminary data on the use of fluorine magnetic resonance spectroscopy (^{19}F-MRS) to assess tissue-engineered islet graft viability by noninvasively measuring oxygen partial pressure (pO_2 or P), and using these measurements to estimate oxygen consumption rate (OCR).

METHODS

Engineered Scaffold Design and Fabrication

Human islets isolated at the University of Pennsylvania were shipped to our institution (as part of the Integrated Islet Distribution Program) following 3 days of postisolation culture. Upon arrival, islets were transferred into silicone rubber membrane culture flasks (Wilson-Wolf Manufacturing Corp, New Brighton, Minn, USA) for culture at 22°C in 5% CO_2 for an additional 2 days. On the day of experimentation, approximately 14,000 islet equivalents (IE) aliquoted into a 15-mL conical tube (BD Biosciences, Franklin Lakes, NJ, USA) were allowed to settle by gravity. After decanting the supernatant, the islet pellet was reconstituted in fresh CMRL 1066 culture media (Mediatech, Inc, Manassas, Va, USA) supplemented with HEPES buffer, heparin, and human serum albumin at a total suspension volume of 180 μL. Engineered scaffolds were constructed by combining fresh commercially available porcine plasma (Sigma-Aldrich, St Louis, Mo, USA) dissolved in calcium-free Krebs buffer solution, 30% v/v perfluorodecalin (PFD; Fluoromed, L.P., Round Rock, Tex, USA), and varying volumes of well-mixed islet suspension (amounting to 2000, 4000, and 8000 IE) in 3.5-cm-diameter Petri dishes (~10 cm^2 area), mixing, and then cross-linking

using 5% v/v topical bovine thrombin solution (King Pharmaceuticals, Bristol, Tenn, USA; 1000 U/mL). Each scaffold had an approximate thickness of 0.3 cm and was covered with 1 mL of culture media. An additional control scaffold was constructed in the same manner only without the addition of an islet suspension. The grafts were cultured at 37°C for a few hours prior to experimentation to allow the oxygen profiles to reach steady state.

Fluorine Magnetic Resonance Spectroscopy

^{19}F-MRS spectra were obtained at 5T using an APOLLO spectrometer (Tecmag Inc, Houston, Tex, USA) with a custom-built single-loop surface coil. Each sample was placed on top of the surface coil and centered within the bore of the magnet. Temperature was controlled using a custom-built water jacket; all measurements were performed at 37°C. A standard inversion recovery sequence was used to estimate ^{19}F spin lattice relaxation time (T1) values corresponding to inversion of the singlet peak in the PFD spectrum. Data were obtained using the NTNMR software (Tecmag Inc) and inversion recovery curves were fit using a custom routine generated in Matlab R2008a v 7.6.0 (Mathworks, Natick, Mass, USA). Equation 1 represents the generalized solution to the Bloch equation for relaxation of longitudinal magnetization (M_z), where *A*, *B*, and T1 are fitting constants that are obtained from the analysis and *t* is the time.

$$M_z = A \cdot \left(1 - 2e^{-t/T1}\right) + B \quad (1)$$

The characteristic T1 for each of the conditions was converted to a steady-state average pO_2 estimate (in the scaffold) using a previously determined linear calibration (pO_2 (mm Hg) = $8.96 \cdot 10^5$/T1 (ms) –213; R^2 = 1.000). Each scaffold was assessed in replicate (n = 6–8).

Mathematical Modeling

The graft was modeled at steady state and as a diffusion-reaction system seeded with a known volume fraction of homogeneously distributed oxygen-consuming tissue. Oxygen was assumed to diffuse from the ambient air at the surface of the media layer (P_A = 160 mm Hg at x = 0 cm). Since the Petri dish is impermeable to gas transport, a zero, flux boundary condition was imposed at the bottom of the scaffold material ($dP/dx = 0$ at $x = 0.4$ cm). Each graft was modeled as a one-dimensional slab of engineered tissue with constant thickness. It was assumed that the islet tissue consumed oxygen with zero-order kinetics, which has been shown to be a reasonable assumption for most conditions involving pO_2 >> Michaelis-Menten constant, Km ~ 0.5 mm Hg.[36,37]

Assuming that no anoxic core develops at the bottom of the scaffold (which was warranted by the tissue volume fractions used), the generalized solution to estimate the volumetric OCR (mol/(cm^3 · s)) is shown by Equation 2, where P_A (mm Hg) is the ambient (surface) pO_2; P_s (mm Hg) is the average steady-state scaffold pO_2 (obtained from ^{19}F-MRS); L_M (cm) is the thickness of media; L_S (cm) is the thickness of the scaffold; ε (dimensionless) is the islet volume fraction in the scaffold; $(\alpha D)_M$ (mol/(cm · s · mm Hg)) is the permeability of oxygen in culture media at 37°C, and $(\alpha D)_s$ (mol/(cm · s · mm Hg)) is the effective permeability of oxygen in the scaffold at 37°C.[36]

$$OCR = \frac{P_A - P_S}{\left(\frac{L_S \cdot L_M}{(\alpha D)_M} + \frac{L_{S^2}}{3(\alpha D)_S}\right)\varepsilon} \quad (2)$$

The effective permeability of oxygen in the scaffold was estimated using the Maxwell relationship,[36] which accounts for the contribution of the dispersed phase (ie, PFD) to the overall permeability. This adjustment is important given the high oxygen solubility of perfluorocarbons. The islet volume fraction estimated from the islet volume and the scaffold volume[38] was calculated by Equation 3, where N_{IE} is the total number of IE per scaffold, R_{IE} (cm) is the radius of an IE, and R_S (cm) is the radius of the cylindrically shaped scaffold.

$$\varepsilon = \frac{4R_{IE^3}N_{IE}}{3R_{S^2}L_S} \quad (3)$$

The volumetric OCR in units of mol/(cm^3 · s) (from Equation 2) can be converted using Equation 4 to an OCR normalized to DNA in units of nmol/(min · mg DNA), which are the standard units of OCR/DNA and a routinely measured islet quality readout in our laboratory,[32,33,35] by assuming a DNA content per IE of DNA_{IE} = 10.4 ng/IE:[38]

$$OCR/DNA = OCR\frac{4\pi}{3}\left(75 \cdot 10^{-4}\right)^3 \frac{60 \cdot 10^6 \cdot 10^9}{10.4} \sim OCR\left(1.0195 \cdot 10^{10}\right) \quad (4)$$

Table 1 summarizes the values of constant parameters used in the theoretical diffusion-reaction model. Figure 1 illustrates a schematic of the theoretical model system, highlighting key dimensions and boundary conditions.

RESULTS

Scaffolds exhibited an IE dose-dependent increase in T1 with a corresponding decrease in steady-state pO_2 estimates (Table 2). From the difference between scaffold pO_2 measurements and ambient pO_2 ($P_A - P_S$), we calculated the islet preparation OCR to be 95 ± 12 (mean ± standard error of the mean, nmol/(min · mg DNA)) using the aforementioned equations. This value compared well with OCR values measured using established methods for' human islet preparations.[33]

DISCUSSION

Engineered strategies for extrahepatic ITx provide appealing alternatives to intraportal infusion, which is the currently performed clinical protocol. Despite the optimism, localized transplantation of a graft seeded with islets has not progressed to clinical application, partly due to: (1) inadequate consideration of oxygen diffusion limitations in the early posttransplant period; (2) a lack of available tools for accurate, quantitative, and noninvasive assessment of tissue-engineered islet graft quality; and (3) failure to appreciate the problems associated with scaling up designs that work well in rodents but require much larger volumes in larger mammals. These data represent preliminary results to develop ^{19}F-MRS as a technique enabling noninvasive quality assessment of tissue-engineered grafts based on direct measurements of pO_2 and estimates of OCR.

Given the inherent inaccuracies of visual counts and with aliquoting islets from preparations, it is important that future studies use more accurate measures (eg, spectrofluorometric DNA quantification) to determine the amount of islet tissue seeded into scaffolds. Additionally, comparisons between direct measurements of islet OCR/DNA (using standard methods[32,33,35]) prior to seeding into scaffolds will enable validation of the ^{19}F-MRS method. Future work may also involve comparing analytical calculations of OCR with solutions generated using finite element methods that relax the homogeneity assumption. It is expected that these types of simulations would yield more accurate estimates of OCR, yet may require a more complete understanding of the spatial distribution of islets within the scaffold, particularly in the direction of oxygen diffusion. Nevertheless, this study highlights the prospective utility of ^{19}F-MRS to measure islet viability at any point following graft construction, which includes during culture and possibly engraftment. ^{19}F-MRS may guide development of new engineered approaches to ITx by enabling meaningful graft monitoring before and after transplantation.

In conclusion, ^{19}F-MRS estimates the amount of viable, oxygen-consuming tissue in a scaffold allowing noninvasive pre- and possibly posttransplant assessment of tissue-engineered islet graft viability.

ACKNOWLEDGMENTS

The authors would like to thank the University of Pennsylvania and the Integrated Islet Distribution Program for supplying the islets used in this study. Additional thanks to all members of the Schulze Diabetes Institute for their thoughtful discussions, especially Dr Louis Kidder, Dr Michael Rizzari, Rebecca Hooper, Jennifer Kitzmann, Kathryn Mueller, William Scott III, Garrett Swindlehurst, Jikku Thomas, and Bradley Weegman.

This work was supported in part by funding from the Iacocca Foundation, the Schott Foundation, the Minnesota Lion Diabetes Foundation, and the National Institute of Diabetes and Digestive and Kidney Diseases SBIR Phase II (R44 DK069865).

REFERENCES

1. Hering BJ, Kandaswamy R, Ansite JD, et al. Single-donor, marginal-dose islet transplantation in patients with type 1 diabetes. JAMA. 2005; 293:830. [PubMed: 15713772]
2. Ryan EA, Shapiro AJ. A patient with severe, recurrent hypoglycemia and glycemic lability who underwent islet transplantation. Nat Clin Pract Endocrinol Metab. 2006; 2:349. quiz 354. [PubMed: 16932312]
3. Gangemi A, Salehi P, Hatipoglu B, et al. Islet transplantation for brittle type 1 diabetes: the UIC protocol. Am J Transplant. 2008; 8:1250. [PubMed: 18444920]
4. Shapiro AM, Ricordi C, Hering BJ, et al. International trial of the Edmonton protocol for islet transplantation. N Engl J Med. 2006; 355:1318. [PubMed: 17005949]
5. Bellin MD, Kandaswamy R, Parkey J, et al. Prolonged insulin independence after islet allotransplants in recipients with type 1 diabetes. Am J Transplant. 2008; 8:2463. [PubMed: 18808408]
6. Koh A, Imes S, Kin T, et al. Supplemental islet infusions restore insulin independence after graft dysfunction in islet transplant recipients. Transplantation. 2010; 89:361. [PubMed: 20145529]
7. Koh A, Senior P, Salam A, et al. Insulin-heparin infusions peritransplant substantially improve single-donor clinical islet transplant success. Transplantation. 2010; 89:465. [PubMed: 20177350]
8. Posselt AM, Bellin MD, Tavakol M, et al. Islet transplantation in type 1 diabetics using an immunosuppressive protocol based on the anti-LFA-1 antibody efalizumab. Am J Transplant. 2010; 10:1870. [PubMed: 20659093]

9. Bellin MD, Sutherland DE, Beilman GJ, et al. Similar islet function in islet allotransplant and autotransplant recipients, despite lower islet mass in autotransplants. Transplantation. 2011; 91:367. [PubMed: 21228753]
10. Rafael E, Tibell A, Ryden M, et al. Intramuscular autotransplantation of 2 pancreatic islets in a 7-year-old child: a 2-year follow-up. Am J Transplant. 2008; 8:458. [PubMed: 18093267]
11. Berman DM, O'Neil JJ, Coffe LC, et al. Long-term survival of nonhuman primate islets implanted in an omental pouch on a biodegradable scaffold. Am J Transplant. 2009; 9:91. [PubMed: 19133931]
12. Shapiro AM, Gallant H, Hao E, et al. Portal vein immunosuppressant levels and islet graft toxicity. Transplant Proc. 1998; 30:641. [PubMed: 9532212]
13. Desai NM, Goss JA, Deng S, et al. Elevated portal vein drug levels of sirolimus and tacrolimus in islet transplant recipients: local immunosuppression or islet toxicity? Transplantation. 2003; 76:1623. [PubMed: 14702535]
14. Tamura K, Fujimura T, Tsutsumi T, et al. Transcriptional inhibition of insulin by FK506 and possible involvement of FK506 binding protein-12 in pancreatic beta-cell. Transplantation. 1995; 59:1606. [PubMed: 7539960]
15. Paty BW, Harmon JS, Marsh CL, et al. Inhibitory effects of immunosuppressive drugs on insulin secretion from HIT-T15 cells and Wistar rat islets. Transplantation. 2002; 73:353. [PubMed: 11884930]
16. Bell E, Cao X, Moibi JA, et al. Rapamycin has a deleterious effect on MIN-6 cells and rat and human islets. Diabetes. 2003; 52:2731. [PubMed: 14578291]
17. Laugharne M, Cross S, Richards S, et al. Sirolimus toxicity and vascular endothelial growth factor release from islet and renal cell lines. Transplantation. 2007; 83:1635. [PubMed: 17589348]
18. Bennet W, Sundberg B, Groth CG, et al. Incompatibility between human blood and isolated islets of Langerhans: a finding with implications for clinical intraportal islet transplantation? Diabetes. 1999; 48:1907. [PubMed: 10512353]
19. Bennet W, Sundberg B, Lundgren T, et al. Damage to porcine islets of Langerhans after exposure to human blood in vitro, or after intraportal transplantation to cynomologus monkeys: protective effects of sCR1 and heparin. Transplantation. 2000; 69:711. [PubMed: 10755515]
20. Goto M, Tjernberg J, Dufrane D, et al. Dissecting the instant blood-mediated inflammatory reaction in islet xenotransplantation. Xenotransplantation. 2008; 15:225. [PubMed: 18957045]
21. Thomas F, Wu J, Contreras JL, et al. A tripartite anoikis-like mechanism causes early isolated islet apoptosis. Surgery. 2001; 130:333. [PubMed: 11490368]
22. Pinkse GG, Bouwman WP, Jiawan-Lalai R, et al. Integrin signaling via RGD peptides and anti-beta1 antibodies confers resistance to apoptosis in islets of Langerhans. Diabetes. 2006; 55:312. [PubMed: 16443762]
23. Tygstrup N, Winkler K, Mellemgaard K, et al. Determination of the hepatic arterial blood flow and oxygen supply in man by clamping the hepatic artery during surgery. J Clin Invest. 1962; 41:447. [PubMed: 13923352]
24. Arteel GE, Thurman RG, Yates JM, et al. Evidence that hypoxia markers detect oxygen gradients in liver: pimonidazole and retrograde perfusion of rat liver. Br J Cancer. 1995; 72:889. [PubMed: 7547236]
25. Sekine N, Cirulli V, Regazzi R, et al. Low lactate dehydrogenase and high mitochondrial glycerol phosphate dehydrogenase in pancreatic beta-cells. Potential role in nutrient sensing. J Biol Chem. 1994; 269:4895. [PubMed: 8106462]
26. Papas KK, Colton CK, Gounarides JS, et al. NMR spectroscopy in beta cell engineering and islet transplantation. Ann N Y Acad Sci. 2001; 944:96. [PubMed: 11797699]
27. Giuliani M, Moritz W, Bodmer E, et al. Central necrosis in isolated hypoxic human pancreatic islets: evidence for postisolation ischemia. Cell Transplant. 2005; 14:67. [PubMed: 15789664]
28. Papas KK, Suszynski TM, Colton CK. Islet assessment for transplantation. Curr Opin Organ Transplant. 2009; 14:674. [PubMed: 19812494]
29. Wang W, Upshaw L, Strong DM, et al. Increased oxygen consumption rates in response to high glucose detected by a novel oxygen biosensor system in non-human primate and human islets. J Endocrinol. 2005; 185:445. [PubMed: 15930171]

30. Fraker C, Timmins MR, Guarino RD, et al. The use of the BD oxygen biosensor system to assess isolated human islets of langerhans: oxygen consumption as a potential measure of islet potency. Cell Transplant. 2006; 15:745. [PubMed: 17269445]
31. Sweet IR, Gilbert M. Contribution of calcium influx in mediating glucose-stimulated oxygen consumption in pancreatic islets. Diabetes. 2006; 55:3509. [PubMed: 17130499]
32. Papas KK, Pisania A, Wu H, et al. A stirred microchamber for oxygen consumption rate measurements with pancreatic islets. Biotechnol Bioeng. 2007; 98:1071. [PubMed: 17497731]
33. Papas KK, Colton CK, Nelson RA, et al. Human islet oxygen consumption rate and DNA measurements predict diabetes reversal in nude mice. Am J Transplant. 2007; 7:707. [PubMed: 17229069]
34. Sweet IR, Gilbert M, Scott S, et al. Glucose-stimulated increment in oxygen consumption rate as a standardized test of human islet quality. Am J Transplant. 2008; 8:183. [PubMed: 18021279]
35. Papas KK, Colton CK, Qipo A, et al. Prediction of marginal mass required for successful islet transplantation. J Invest Surg. 2010; 23:28. [PubMed: 20233002]
36. Avgoustiniatos ES, Colton CK. Effect of external oxygen mass transfer resistances on viability of immunoisolated tissue. Ann N Y Acad Sci. 1997; 831:145. [PubMed: 9616709]
37. Avgoustiniatos, ES.; Colton, CK. Design considerations in immunoisolation.. In: Landes, RG.; Lanza, RP.; Langer, R.; Chick, WL., editors. Principles of Tissue Engineering. Austin, Tex: 1997. p. 333
38. Colton, CK.; Papas, KK.; Pisania, A., et al. Characterizations of Islet Preparations, Cellular Transplantation: From Laboratory to Clinic. Academic Press; San Diego: 2007. p. 85

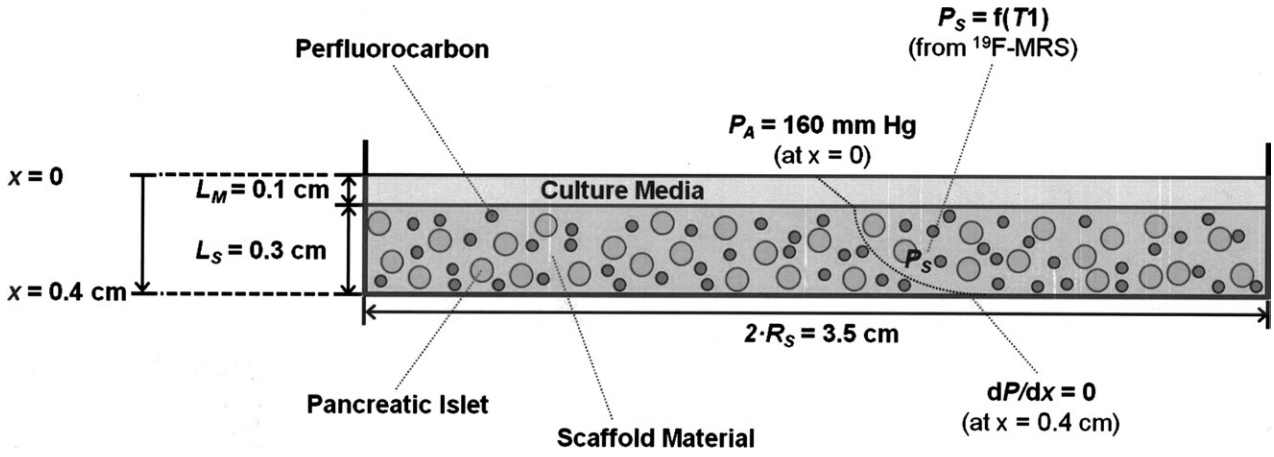

Fig 1.

Schematic illustrating the generalized design of the tissue-engineered graft containing scaffold material (cross-linked plasma), emulsified perfluorocarbon (represented by the smaller, darker circles) and human pancreatic islets (represented by the larger, lighter circles), and also highlighting boundary conditions used in the diffusion-reaction model. Symbols presented in this figure are defined in the Mathematical Modeling subsection of the Methods. ^{19}F-MRS, fluorine magnetic resonance spectroscopy; L_M, thickness of culture media layer; L_S, thickness of scaffold; P_A, ambient (and media surface) oxygen partial pressure (pO_2); P_S, average scaffold pO_2; T1, spin lattice relaxation time; R_S, radius of cylindrically shaped scaffold.

Table 1

Values of Constants Used for Theoretical Modeling

Constant	Units	Value	Reference
P_A	mm Hg	160	—
L_M	cm	0.1	—
L_S	cm	0.3	—
$(\alpha D)_M$	mol/(cm · s · mm Hg)	$3.53 \cdot 10^{-14}$	36
$(\alpha D)_S$	mol/(cm · s · mm Hg)	$7.06 \cdot 10^{-14}$	36
R_S	cm	1.75	—
R_{IE}	cm	0.0075	—
N_{IE}	—	2000, 4000, 8000	—
DNA_{IE}	ng	10.4	38

P_A, ambient (or surface) oxygen partial pressure (pO_2); L_M, thickness of culture media layer; L_S, thickness of scaffold; $(\alpha D)_M$, oxygen permeability in culture media; $(\alpha D)_S$, oxygen permeability in scaffold; R_S, radius of scaffold; R_{IE}, radius of islet equivalent (IE); N_{IE}, number of IE seeded into scaffold; DNA_{IE}, DNA content per IE.

Table 2

T1 Values (mean ± SEM) and pO_2 Estimates for Scaffolds Seeded With Varying Numbers of IE (n = 6–8 for Each Condition)

IE per Scaffold	T1 Measured (ms)	pO_2 Estimate, P_s (mm Hg)
0	1866 ± 7	160
2000	1942 ± 9	145
4000	2081 ± 11	121
8000	2181 ± 15	106

IE, islet equivalent; pO_2, oxygen partial pressure; P_S, scaffold pO_2; SEM, standard error of the mean; T1, spin lattice relaxation time.